On Intuitive Control of Ankle-Foot Prostheses: A Sensor Fusion-based Algorithm for Real-Time Prediction of Transitions to Compliant Surfaces

Charikleia Angelidou and Panagiotis Artemiadis*, *IEEE Senior Member*

***Abstract*— Substantial research and development on the design and control of robotic ankle-foot prostheses have aimed to restore normal function and movement capacity for people with gait impairments and lower limb amputations. However, prostheses controllers usually fail to incorporate information pertaining to the properties of the walking terrain, such as ground stiffness. There is therefore a need for a framework that adjusts the prostheses parameters according to the user's intent to transition to a variable impedance terrain. To achieve this, we need to incorporate the human wearer in the control loop of the prosthesis. This work proposes an advanced, high-level controller framework for powered ankle-foot prostheses that combines subject-specific pattern recognition (PR) and classification strategies to predict whether the next step will be on a rigid or compliant surface. Comparing the Support Vector Machine (SVM) and k-Nearest Neighbors (k-NN) classification algorithms for this task, we conclude that by combining a k-NN implementation with a Pattern Recognition Neural Network (PR NN), our method can accurately forecast upcoming surface stiffness transitions in time to allow for prompt adaptation to the new walking terrain. We also show that the sensor fusion of kinematic and surface electromyographic (EMG) data outperforms single-source inputs producing the best prediction results for all subjects with an accuracy of up to 87.5%.**

I. Introduction

A significant part of a person's daily locomotion consists of walking on dynamic terrains and transitions between inhomogeneous, uneven surfaces. Proprioception - a mechanism that is activated before each movement is carried out [1] - allows healthy individuals to forecast their next move and adapt their gait to the new walking surface. However, agility and walking stability on non-flat and compliant surfaces pose major challenges for people with lower limb amputations [2,3]. It is thus essential to enable prosthesis/orthosis wearers to smoothly ambulate and adapt to dynamic environments by transfusing the intelligent anticipatory mechanisms of human locomotion into state-of-the-art powered ankle-foot prostheses.

Previous works have focused on expanding the real-world viability of prosthetic devices by developing strategies to coordinate the robotic prosthesis movements with the user's neuromuscular system and enable them to transition between different daily life activities. Running activities and walking tasks such as avoiding obstacles and alternating between locomotion modes (i.e. level-ground walking to stair ascend) have been the center of focus when it comes to early lower-limb muscle activation [4, 5]. These works on anticipation and user intent prediction mainly use EMG [6,7], mechanical data [8] or multisensory fusion [9–11]. Most recent works also study the use of sonomyography to classify and distinguish between different ambulation modes [12, 13]. Results of these studies have shown that by combining data from different sources it is possible to achieve higher prediction accuracy than by using either data source separately [14].

Early muscle activation during transitions from rigid to compliant surfaces has been studied in works that reveal the existence of anticipatory muscle responses for both legs just before and immediately after an individual encounters a compliant surface [15–17]. However, in spite of current progress in the development of user-intuitive prostheses for transitioning between locomotion modes, characteristic biosignals, and other available data sources for the identification of user intent when transitioning from rigid to compliant surfaces have only recently been explored [18].

Our goal is to further expand on this first successful attempt to address robust walking over dynamic terrains for people with gait impairments or lower-limb amputation and study the use of different data source signals as inputs to the proposed phase-dependent, subject-specific pattern recognition (PR) and classification algorithm for identifying cases of transversing rigid and compliant terrains (see Fig. 1). Specifically, in this paper we compare the performance of the proposed strategy when the data input consists of only the surface EMG signals or kinematic data or a fusion of the two. The performance results confirm that data fusion is able to achieve higher accuracy than data from a single source, proving that kinematics and EMG data fusion is both feasible and efficient for the control of lower-limb prostheses.

II. methods

A. Experimental Protocol

Eight healthy subjects (age 26.6 $\pm$ 2.2 years, height 174.2 $\pm$ 8.7 cm, mass 70.8 $\pm$ 12.3 kg) were recruited to walk on a unique robotic platform, the Variable Stiffness Treadmill (VST) [19–21]. For the data collection, the subjects chose a comfortable walking speed that closely resembled their normal, everyday walking patterns. After different treadmill speeds between 70 and 100 cm/s were tested, all 8 subjects chose to walk at 90 cm/s. All participants completed a total of 554 gait cycles (GCs), which correspond to approximately 12 minutes of treadmill walking with a belt speed of 90 cm/s.

*This material is based upon work supported by the National Science Foundation under Grants No. 2020009, 2015786, 2025797, and 2018905.

Charikleia Angelidou and Panagiotis Artemiadis are with the Mechanical Engineering Department, at the University of Delaware, Newark, DE 19716, USA. cangelid@udel.edu, partem@udel.edu

*Corrresponding author

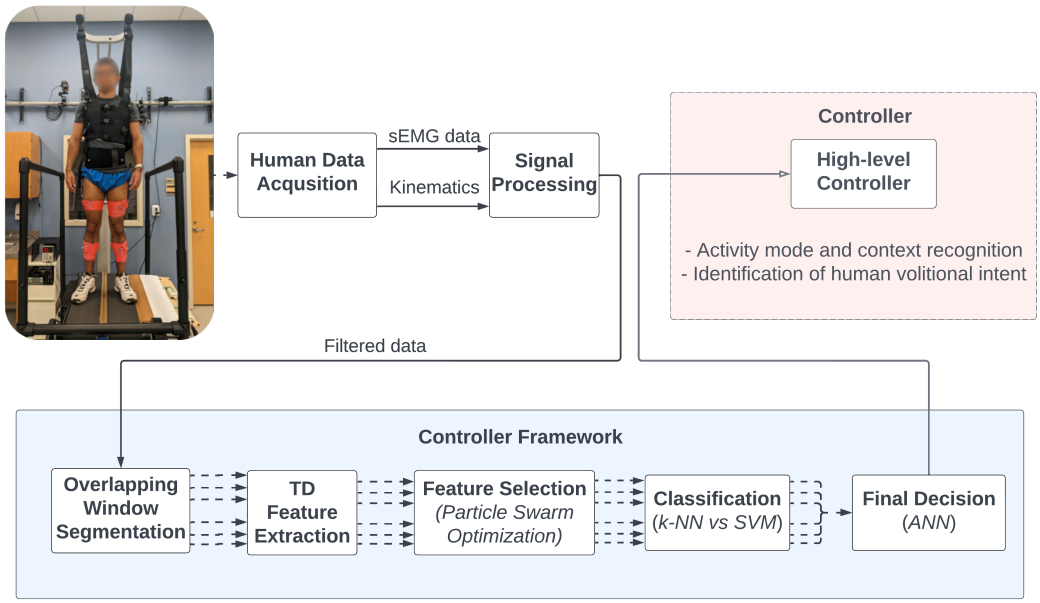

Fig. 1: Flowchart of the proposed research strategy. Current work focuses on data acquisition, processing and controller framework development. The *Controller* block of the flowchart is not included in the analysis.

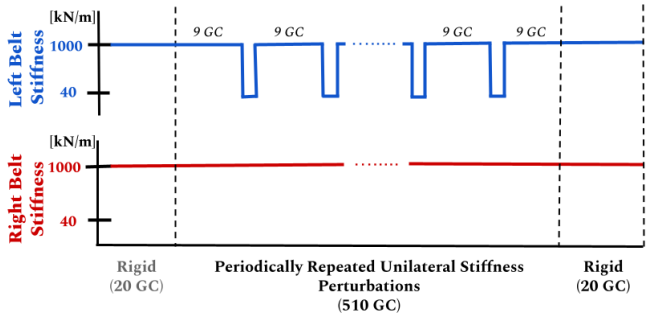

Fig. 2: Visual schematic of the experimental protocol. The surface stiffness of the left belt dropped from 1000 kN/m (rigid) to 40 kN/m (compliant) periodically every 10 gait cycles (GCs) (9 rigid GCs - 1 compliant GC) for a total of 510 GCs. The surface stiffness of the right belt was always 1000 kN/m (i.e. rigid ground). The first 20 rigid surface gait cycles were precluded from the data processing and analysis.

Transitions between surfaces are assumed to be first experienced by one – the leading – leg, which for our study was the left leg. Therefore, expected stiffness perturbations, which the subjects were verbally informed of ahead of time, were applied unilaterally to the left leg, while the right leg was stepping on a rigid surface throughout the whole experiment (Fig. 2). The experimental protocol was approved by the University of Delaware Institutional Review Board (IRB ID# 1544521-7) and informed consent from the subjects was obtained at the time of the experiment.

In terms of kinematics, data were recorded by placing 23 reflective motion capture markers on the subjects' lower limbs and torso. All kinematic data were sampled at a 100 Hz frequency and synchronized with the recorded muscular activity using the real-time *Foot VErtical & Sagittal Position Algorithm (F-VESPA)* for heel-strike detection [22].

Muscle activity was measured with 12 wireless surface EMG sensors (Trigno, Delsys Inc.) from six major muscles of both legs: the tibialis anterior (TA), gastrocnemius (GA), soleus (SOL), rectus femoris (RF), vastus lateralis (VL), and biceps femoris (BF). These muscles were selected due to their major power-generating function and their fundamental role in ankle motion and stability. EMG data were sampled at a 2 kHz frequency. After computing the EMG linear envelope, the data were normalized to the maximum activation value of each muscle. The gait cycles were categorized into Rigid (R) and Transition (T) GCs according to whether the subject was preparing to step on a rigid or a compliant surface respectively. The perturbation gait cycles, as well as one gait cycle following each perturbation, were removed from the dataset. Running an outlier detection method for periodic data [23] on the remaining GCs, outlier gait cycles were identified and removed from the dataset.

B. Data Analysis

The proposed controller framework is schematically presented in Fig. 1. Each process block comprising the framework is thoroughly described in [18] and summarized in this work for brevity purposes.

1) Overlapping Window Segmentation: We employed the idea of a phase-dependent analysis, by applying a sliding window approach on both the EMG and kinematic data. The input signals were segmented into 50% overlapping windows of 150ms. The windowing partition was applied only to the data between the Left Toe-Off (LTO) and Left Heel-Strike (LHS) gait events, yielding a total of six analysis windows per GC (Fig. 3). This choice was based on our hypothesis that the prediction performance of a classifier will increase as the gait cycle progresses and the subjects prepare to step on a compliant surface.

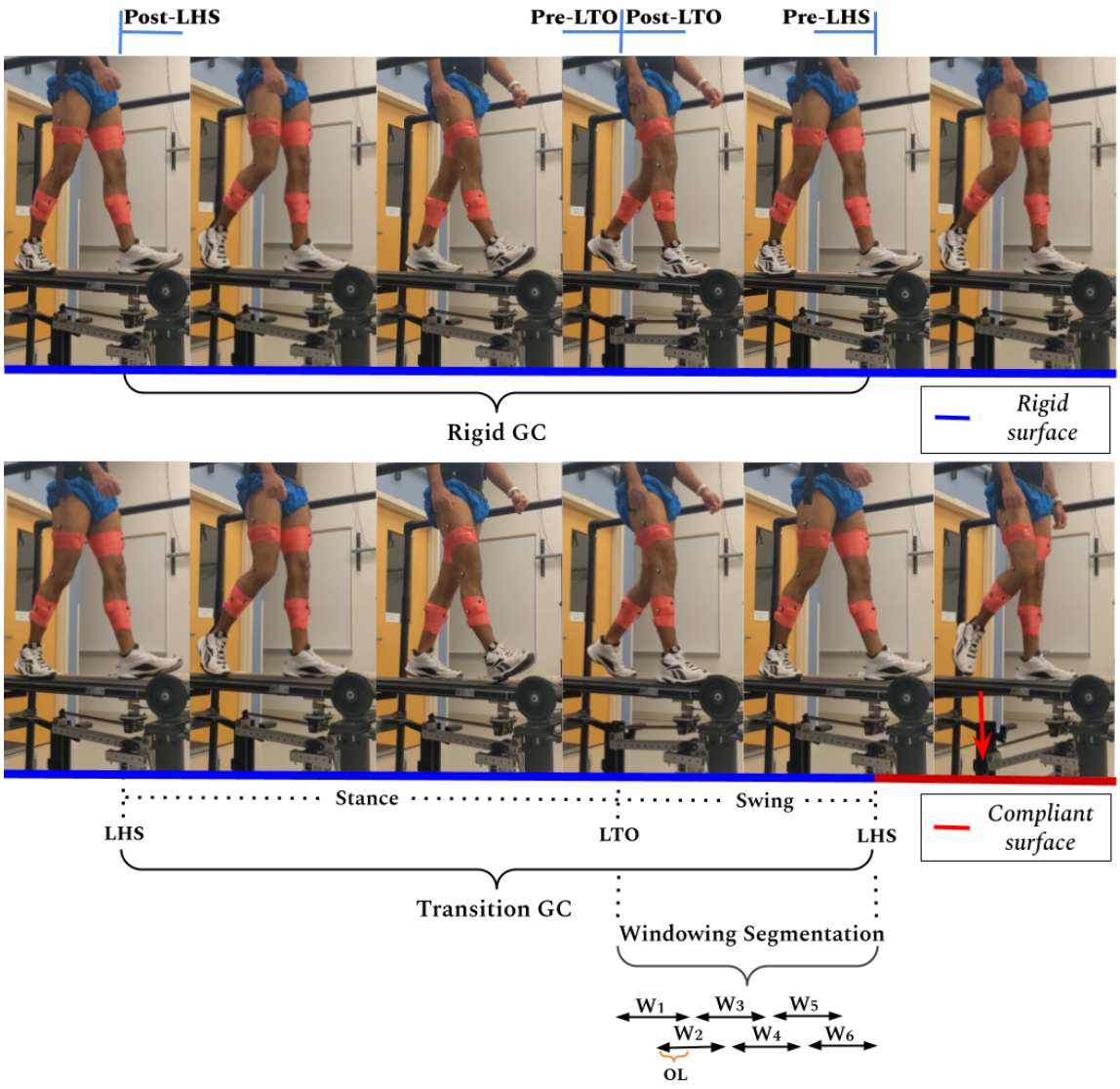

Fig. 3: Representative subject walking on the VST. Each gait cycle begins and ends at Left Heel Strike (LHS). Gait cycles were categorized into Rigid (R) and Transition (T) GCs according to whether the subject was preparing to step on a rigid (top) or a compliant (bottom) surface respectively. The red arrow indicates the vertical deflection of the VST to simulate a compliant surface. The continuous windowing segmentation is schematically presented. The six overlapping (OL = 50%) windows ($W_1, W_2, ..., W_6$) are aligned with the respective LTO and LHS gait events.

2) Feature Extraction & Selection: Feature extraction and selection was carried out in the time domain (TD) to fulfill the fast time-response requirement of real-time systems.

a) EMG Features: EMG features were extracted from six muscles of both lower limbs, which included the TA, VL, BF, and RF of the left leg, and the SOL, and GA of the right leg. The SOL and GA of the left leg, as well as the TA, VL, BF, and RF of the right leg were excluded from the analysis due to their lack of substantial activation after the Pre-LTO phase. For each window, we extracted 12 features per muscle, which corresponds to a total of 72 EMG features per segmented window. The extracted features included the Mean Absolute Value, Waveform Length, Difference Variance Value, Root Mean Square, Simple Square Integrated, Integrated EMG, Variance of EMG, Difference Absolute Mean Value, Standard Deviation, Average Amplitude Change, Kurtosis, and Skewness.

b) Kinematic Features: In terms of kinematics, the features extracted were the maximum, mean, and minimum values of the leg joint angles including the flexion/extension of the hip, knee, and ankle of both legs, as well as the angular velocity of the latter two joints. We extracted a total of 30 kinematic features per segmented window, which correspond to 3 features for each of the 10 kinematic variables studied.

c) EMG & Kinematic Features Fusion: Combining the feature extraction processes followed for the distinct EMG and kinematic cases respectively, the result is a $72+30 = 102$ (features) $\times$ 6 (windows) = 612 elements wide feature vector per GC and subject. The extracted features were organized in a single, window-specific feature vector.

To preserve the important features of the dataset but decrease the complexity of the system, we employed a

wrapper feature selection method called Particle Swarm Optimization (PSO) [24] to select a subset of relevant features to use in our classification model for faster and more accurate predictions. Details on parameter selection and algorithm application are analytically presented in our previous work on gait classification on compliant surfaces [18].

3) Classification and PR Strategy: We suggest that a classification algorithm can be trained to differentiate between rigid and compliant surface transitions when a sufficient set of feature inputs is provided. In this paper, the feature inputs tested for each window classifier consist of 1) kinematics only, 2) EMG only, and 3) EMG & kinematics fusion signals. In addition to studying the effect of the feature input on classifier performance, the present study also compares the efficiency of the k-Nearest Neighbors (k-NN) and Support Vector Machine (SVM) algorithms to identify and classify walking patterns on transitions between surfaces of variable stiffness. Our goal is to classify gait cycles into two class labels according to whether the transition happens on: (1) rigid-rigid (R), and (2) rigid-compliant surface (T) (Fig. 3).

a) k-NN: The k-NN algorithm is a supervised learning classifier, which uses proximity to classify and predict the group an individual data point belongs to. Our k-NN algorithm utilizes $k = 9$ nearest neighbors. For our algorithm implementation, the built-in Matlab function *fitcknn()* was used, implementing a Euclidean distance metric d in combination with an inverse distance weight ($w = \frac{1}{d}$).

b) SVM: An SVM classifies data by finding the best hyperplane that separates all data points of one class from those of the other class. The support vectors are the data points closest to the separating hyperplane. For algorithm implementation, the built-in Matlab function *fitcsvm()* was used, utilizing a Radial Basis Function (RBF) kernel.

For both k-NN and SVM, the software centered and scaled each predictor variable by the corresponding weighted column mean and standard deviation. Also, it must be noted that the classifiers were trained and applied to each of the six segmented windows, which resulted in six distinct classifier decisions per gait cycle.

c) PR Neural Networks (NN): To combine the distinct decisions of the six window classifiers into a final decision for each gait cycle, we developed a pattern recognition NN. We used the classification training data to extract six binary decisions (R or T for each window) per gait cycle. The binary decisions were then used as the training input to the PR NN. In a similar manner, the testing data used to evaluate the window classifiers were also used for evaluating the performance of the PR NN. For algorithm implementation, the built-in Matlab function *patternnet()* was used with 1 hidden layer of 100 nodes.

4) Performance Evaluation Metrics: In order to evaluate the classification and prediction performance of our high-level control strategy under different inputs and algorithms, we define the *Balanced Accuracy* and *Matthews Correlation Coefficient (MCC)* metrics. MCC ranges between -1 and 1, with 1 representing the perfect classifier and values around 0 representing a random guess classifier.

III. Results

A. Feature Extraction & Selection

Applying the PSO feature selection method, we were able to reduce the dimensionality of each of the input feature vectors. Specifically, the initial feature set pertaining to the EMG data (72 extracted features) and the kinematics data (30 extracted features) was reduced to approximately 21 ± 7 and 6 ± 3 features per window across all subjects, respectively. Similarly, the dimensionality of the feature set for the EMG and kinematics fusion case (102 total features) was reduced to 30 ± 9 for each window.

B. Classification

Our classification strategy was tested using the k-NN and SVM classification algorithms under three different input feature sets: i) kinematics only *(KIN)*, ii) EMG only *(EMG)* and iii) *KIN-EMG fusion*.

a) k-NN: We observe that the Balanced Accuracy metric presents a consistently increasing profile for the case of the KIN-EMG fusion as we approach the end of each gait cycle (yellow bar in Fig. 4), unlike the kinematic and EMG only cases. We specifically observe that the kinematics case (blue bar in Fig. 4) fluctuates between 50.1% and 56.4% throughout the last 5 window classifiers. The EMG case (red bar in Fig. 4) achieves similar accuracy rates with the KIN-EMG fusion, however, the latter is able to outperform the former for the majority of the windows. The performance of the KIN-EMG fusion set peaks in window classifier 6, achieving a subject average accuracy of 71.5%. These findings are also confirmed by studying the MCC behavior of each k-NN classifier across all subjects (Fig. 5). To be more exact, the KIN-EMG fusion shows a robust increasing behavior that achieves higher values compared to KIN or EMG alone. We can therefore deduce that for the k-NN classification algorithm, the KIN-EMG fusion constitutes on average a more efficient source of information to predict transitions between surfaces of variable stiffness.

b) SVM: The results observed for the case of the k-NN classifiers were also replicated for the SVM. Similarly to the k-NN, the kinematic data source consistently generates the lowest classification accuracy among the available data sources (Fig. 6). The EMG and KIN-EMG fusion cases closely resemble each other, with the data fusion once again outperforming the EMG-only case for the majority of the segmented windows. The highest accuracy value achieved by the SVM data fusion was 70.9% in window 5. The superiority of the fusion case can also be confirmed by the average corresponding MCC profiles of each SVM classifier (Fig. 7), which show similar trends as with the k-NN (Fig. 5). It can therefore be concluded that the KIN-EMG fusion indeed yields better prediction rates and classifier performance for the SVM case as well.

Comparing the two algorithms under the KIN-EMG fusion input we observe more stable and consistent results for the

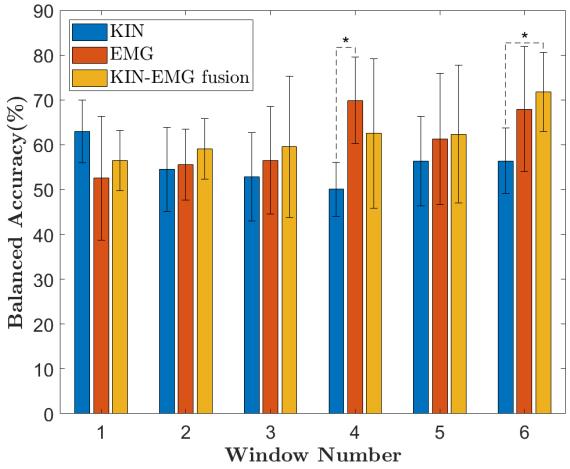

Fig. 4: Performance evaluation of the k-NN algorithm implementation under kinematic (KIN), EMG, and kinematic-EMG (KIN-EMG fusion) input across all subjects. Statistical significance (*) was calculated using an independent 2-sample t-test at the 95% confidence level.

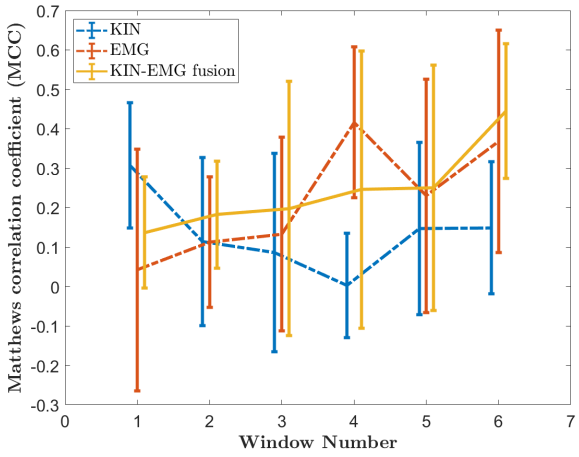

Fig. 5: MCC progression of the k-NN algorithm implementation under KIN, EMG, and KIN-EMG fusion input across all subjects.

case of the k-NN. Specifically, the performance of each k-NN window classifier confirms our initial hypothesis that the prediction accuracy will be higher toward the end of each gait cycle as we approach the last segmented windows. On the other hand, the SVM classifiers seem to fluctuate between the segmented windows, leading to a rather unreliable result when compared to the k-NN algorithm.

In fact, the performance evaluation with our best subject in the case of the k-NN KIN-EMG fusion showed that Balanced Accuracy gradually improved from 45.8% (window 1) to 87.5% (window 6), achieving an impressive increase of 41.7% (Fig. 8), outperforming the respective kinematics input by up to 133.3%.

c) PR NN: Applying the PR NN methodology to the resulting k-NN window classifiers, we shift our focus to serial combinations of windows rather than single window classifiers. Combining the prediction results of each classifier into a final PR NN framework, we observe that the KIN-EMG fusion outperforms its KIN and EMG counterparts by

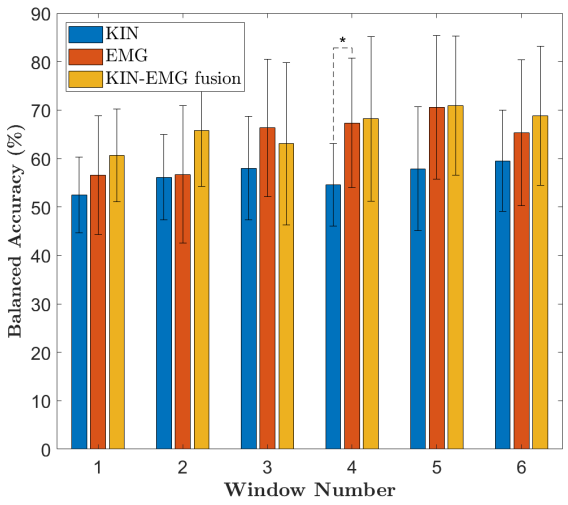

Fig. 6: Performance evaluation of the SVM algorithm implementation under KIN, EMG, and KIN-EMG fusion input across all subjects. Statistical significance (*) was calculated using an independent 2-sample t-test at the 95% confidence level.

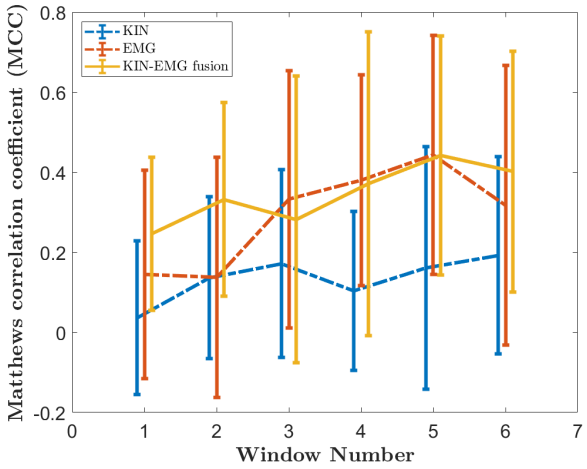

Fig. 7: MCC progression of the SVM algorithm implementation under KIN, EMG, and KIN-EMG fusion input across all subjects.

13.19% and 6.51% respectively (Fig. 9).

IV. Conclusion

This work combines surface EMG signals and kinematic data with a phase-dependent PR algorithm for predicting user intention to step on a rigid or compliant surface. The kinematics-EMG data fusion was able to distinguish between the two cases based exclusively on human user biosignature input, accomplishing up to 87.5% prediction accuracy while outperforming single-source inputs by up to 133.3%.

The benefit of our subject-specific approach is that it is trainable to each subject's signals, taking into account the distinct EMG and kinematic parameters of each individual subject under different surface stiffnesses. Therefore, we support that our framework can be used to generate accurate and comparable predictions about the surface compliance of the user's upcoming step even in populations not tested in this analysis, e.g., transtibial amputees. These predictions

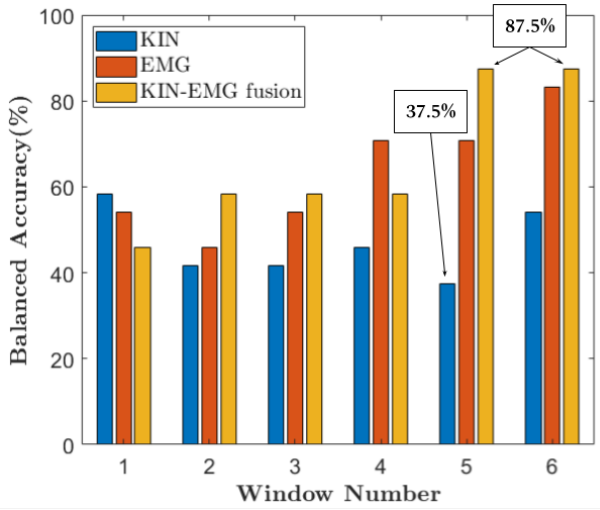

Fig. 8: Performance evaluation for the best subject using k-NN window-classifiers.

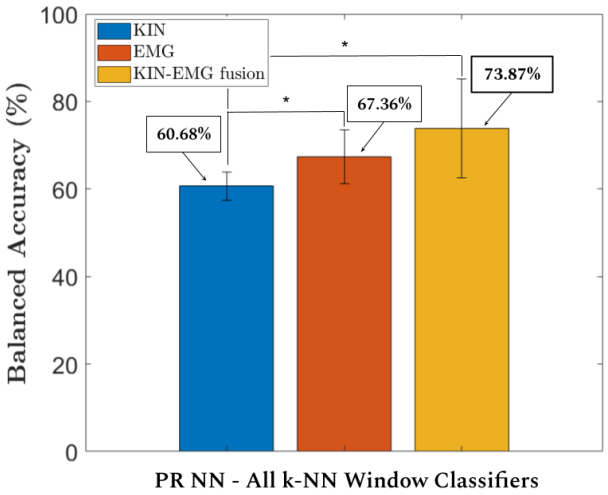

Fig. 9: Performance evaluation of the PR NN implementation under KIN, EMG, and KIN-EMG fusion input across all subjects. Statistical significance (*) was calculated using an independent 2-sample t-test at the 95% confidence level.

can be applied as input to a high-level controller to tune the prosthesis ankle stiffness in real-time. The proposed method can be incorporated into the control architecture of lower limb prostheses to allow for intuitive human-in-the-loop controls that can lead to increased safety, stability, and overall acceptance of the prosthesis.

REFERENCES

[1] M. MacKay-Lyons, "Central pattern generation of locomotion: A review of the evidence," *Physical Therapy*, vol. 82, pp. 69–83, 1 2002.

[2] M. E. V. D. Berg, C. J. Barr, S. Cavenett, and M. Crotty, "Gait analysis in individuals with transtibial amputation walking on sand: Comparing everyday prosthesis with a water-activity prosthesis," *Journal of Prosthetics and Orthotics*, vol. 32, pp. 107–115, 4 2020.

[3] J. Kim, M. J. Major, B. Hafner, and A. Sawers, "Frequency and circumstances of falls reported by ambulatory unilateral lower limb prosthesis users: A secondary analysis," *PM&R*, vol. 11, pp. 344–353, 4 2019.

[4] D. P. Ferris, K. Liang, and C. T. Farley, "Runners adjust leg stiffness for their first step on a new running surface," *Journal of Biomechanics*, vol. 32, pp. 787–794, 1999.

[5] L. Li and L. L. Ogden, "Muscular activity characteristics associated with preparation for gait transition," *Journal of Sport and Health Science*, vol. 1, pp. 27–35, 5 2012.

[6] H. Huang, T. A. Kuiken, and R. D. Lipschutz, "A strategy for identifying locomotion modes using surface electromyography," *IEEE Transactions on Biomedical Engineering*, vol. 56, pp. 65–73, 1 2009.

[7] S. Huang and D. P. Ferris, "Muscle activation patterns during walking from transtibial amputees recorded within the residual limb-prosthetic interface," *Journal of NeuroEngineering and Rehabilitation*, vol. 9, pp. 1–16, 8 2012.

[8] H. A. Varol, F. Sup, and M. Goldfarb, "Multiclass real-time intent recognition of a powered lower limb prosthesis," *IEEE Transactions on Biomedical Engineering*, vol. 57, p. 542, 3 2010.

[9] H. Huang, F. Zhang, L. J. Hargrove, Z. Dou, D. R. Rogers, and K. B. Englehart, "Continuous locomotion-mode identification for prosthetic legs based on neuromuscular–mechanical fusion," *IEEE Transactions on Biomedical Engineering*, vol. 58, p. 2867, 10 2011.

[10] C. Fang, B. He, Y. Wang, J. Cao, and S. Gao, "Emg-centered multisensory based technologies for pattern recognition in rehabilitation: State of the art and challenges," *Biosensors*, vol. 10, 7 2020.

[11] N. E. Krausz and L. J. Hargrove, "Sensor fusion of vision, kinetics, and kinematics for forward prediction during walking with a transfemoral prosthesis," *IEEE Transactions on Medical Robotics and Bionics*, vol. 3, pp. 813–824, 5 2021.

[12] R. Murray, J. Mendez, L. Gabert, N. P. Fey, H. Liu, and T. Lenzi, "Ambulation mode classification of individuals with transfemoral amputation through a-mode sonomyography and convolutional neural networks," *Sensors*, vol. 22, p. 9350, 12 2022.

[13] K. G. Rabe and N. P. Fey, "Evaluating electromyography and sonomyography sensor fusion to estimate lower-limb kinematics using gaussian process regression," *Frontiers in Robotics and AI*, vol. 9, p. 58, 3 2022.

[14] A. J. Young, T. A. Kuiken, and L. J. Hargrove, "Analysis of using emg and mechanical sensors to enhance intent recognition in powered lower limb prostheses," *Journal of Neural Engineering*, vol. 11, p. 056021, 9 2014.

[15] J. Skidmore and P. Artemiadis, "On the effect of walking surface stiffness on inter-limb coordination in human walking: toward bilaterally informed robotic gait rehabilitation," *Journal of NeuroEngineering and Rehabilitation*, vol. 13, p. 32, 3 2016.

[16] E. Q. Yumbla, R. A. Obeng, J. Ward, T. Sugar, and P. Artemiadis, "Anticipatory muscle responses in transitions from rigid to compliant surfaces: towards smart ankle-foot prostheses," *IEEE International Conference on Rehabilitation Robotics*, vol. 2019, pp. 880–885, 6 2019.

[17] M. Drolet, E. Q. Yumbla, B. Hobbs, and P. Artemiadis, "On the effects of visual anticipation of floor compliance changes on human gait: Towards model-based robot-assisted rehabilitation," *Proceedings - IEEE International Conference on Robotics and Automation*, pp. 9072–9078, 5 2020.

[18] C. Angelidou and P. Artemiadis, "On predicting transitions to compliant surfaces in human gait via neural and kinematic signals," *IEEE Transactions on Neural Systems and Rehabilitation Engineering*, vol. 31, pp. 2214–2223, 2023.

[19] J. Skidmore, A. Barkan, and P. Artemiadis, "Investigation of contralateral leg response to unilateral stiffness perturbations using a novel device," in *2014 IEEE/RSJ International Conference on Intelligent Robots and Systems*, 9 2014, pp. 2081–2086.

[20] A. Barkan, J. Skidmore, and P. Artemiadis, "Variable stiffness treadmill (VST): A novel tool for the investigation of gait," *Proceedings - IEEE International Conference on Robotics and Automation*, pp. 2838–2843, 9 2014.

[21] J. Skidmore, A. Barkan, and P. Artemiadis, "Variable stiffness treadmill (VST): System development, characterization, and preliminary experiments," *IEEE/ASME Transactions on Mechatronics*, vol. 20, 2015.

[22] C. Karakasis and P. Artemiadis, "F-VESPA: A kinematic-based algorithm for real-time heel-strike detection during walking," *IEEE International Conference on Intelligent Robots and Systems*, pp. 5098–5103, 2021.

[23] B. Hobbs and P. Artemiadis, "A systematic method for outlier detection in human gait data," in *2022 International Conference on Rehabilitation Robotics (ICORR)*, 2022.

[24] J. Kennedy and R. Eberhart, "Particle swarm optimization," *Proceedings of ICNN'95 - International Conference on Neural Networks*, vol. 4, pp. 1942–1948, 1995.